Nuclear Instruments and Methods in Physics Research B 384 (2016) 113–120

Contents lists available at ScienceDirect

Nuclear Instruments and Methods in Physics Research B

journal homepage: www.elsevier.com/locate/nimb

Spatial distributions of dose enhancement around a gold nanoparticle at several depths of proton Bragg peak

Jihun Kwon [a], Kenneth Sutherland [b], Takayuki Hashimoto [c], Hiroki Shirato [d], Hiroyuki Date [e,*]

[a] Department of Radiation Oncology, Hokkaido University Graduate School of Medicine, Hokkaido University, Japan
[b] Department of Medical Physics, Hokkaido University Graduate School of Medicine, Hokkaido University, Japan
[c] Department of Radiation Medicine, Hokkaido University Graduate School of Medicine, Japan
[d] Department of Radiation Medicine, Hokkaido University Graduate School of Medicine and Global Station for Quantum Medical Science and Engineering, Global Institution for Collaborative Research and Education (GI-CoRE), Hokkaido University, Japan
[e] Faculty of Health Sciences, Hokkaido University, Japan

ARTICLE INFO

Article history:
Received 4 June 2016
Received in revised form 10 August 2016
Accepted 22 August 2016
Available online 31 August 2016

Keywords:
Gold nanoparticles
Proton therapy
Radial dose distribution
Monte Carlo simulation
Radiation sensitizer
Dose enhancement

ABSTRACT

Gold nanoparticles (GNPs) have been recognized as a promising candidate for a radiation sensitizer. A proton beam incident on a GNP can produce secondary electrons, resulting in an enhancement of the dose around the GNP. However, little is known about the spatial distribution of dose enhancement around the GNP, especially in the direction along the incident proton. The purpose of this study is to determine the spatial distribution of dose enhancement by taking the incident direction into account. Two steps of calculation were conducted using the Geant4 Monte Carlo simulation toolkit. First, the energy spectra of 100 and 195 MeV protons colliding with a GNP were calculated at the Bragg peak and three other depths around the peak in liquid water. Second, the GNP was bombarded by protons with the obtained energy spectra. Radial dose distributions were computed along the incident beam direction. The spatial distributions of the dose enhancement factor (DEF) and subtracted dose (D_{sub}) were then evaluated. The spatial DEF distributions showed hot spots in the distal radial region from the proton beam axis. The spatial D_{sub} distribution isotropically spread out around the GNP. Low energy protons caused higher and wider dose enhancement. The macroscopic dose enhancement in clinical applications was also evaluated. The results suggest that the consideration of the spatial distribution of GNPs in treatment planning will maximize the potential of GNPs.

1. Introduction

In recent years, proton therapy has been applied as a novel strategy to treat cancer. Protons penetrate to a particular depth of matter depending on their initial energy, and lose most of their energy around the end of their range forming the "Bragg peak". This unique physical characteristic enables us to concentrate the dose on the tumor while sparing the dose to normal tissues. In this way, proton therapy realizes a better dose distribution compared to conventional X-ray radiotherapy. However, the total amount of radiation exposure is still limited in order to avoid the induction of harmful side effects. For this reason, the utilization of gold nanoparticles (GNPs) has been examined as a candidate radiation sensitizer to enhance the therapeutic effects of radiation at the treatment target.

GNPs possess some beneficial features. They are not harmful chemically to the patient since gold (Au) is an inert and biocompatible material [1]. Owing to their multiple surface ligands, GNPs can be chemically bound with antibodies and preferentially accumulate in the tumor for a relatively long time compared to iodine-based contrast agents [2–4]. In addition, because of the high atomic number of gold, radiation incident on GNPs produces many secondary electrons that enhance the dose around every nanoparticle and also creates reactive oxygen species (ROS) by radiolytic processes [5,6].

The investigation of GNPs as a radiation sensitizer began with X-rays. Hainfeld et al. reported the reduction of tumor volume and the prolongation of the survival rate in mice when 1.9 nm GNPs were irradiated by 250 kVp X-rays [4]. GNPs were shown to agglomerate outside of the cell nucleus in most *in vitro* experiments [7,8], while a few reports indicate that GNPs can be targeted inside the cell nucleus [9]. Misawa and Takahashi found an elevation of the ROS generation rate under diagnostic X-ray irradiation

* Corresponding author.
E-mail address: date@hs.hokudai.ac.jp (H. Date).

http://dx.doi.org/10.1016/j.nimb.2016.08.013
0168-583X/

to GNPs [10]. To understand the dosimetric contribution of GNPs, many simulation studies have shown dose enhancement caused by secondary electrons in the vicinity of GNPs. kV X-ray irradiation showed a higher dose enhancement compared to MV X-rays due to the high photoelectric effect cross section in low-energy X-ray irradiation [11–13]. Despite a large number of extensive studies of GNP radiation sensitization using photon beams, reports for proton beams are relatively scarce. With proton beam irradiation, GNPs may dramatically improve the treatment outcomes around the Bragg peak region. A few *in vitro* studies have revealed that GNPs can increase cell killing with proton beams as well as with X-rays [14,15]. The prolongation of the survival rate of tumor embedded mice under proton irradiation was demonstrated to be a result of ROS generation [16]. Furthermore, Monte Carlo simulations have shown that a large number of electrons are emitted from GNPs under proton irradiation [17].

To evaluate the radiation sensitizing effect with GNPs, it is essential to estimate the dose distribution around a GNP sphere. In this respect, some studies have focused on the radial dose distributions around the GNP [11,18,19]. Jones et al. calculated the radial dose distributions under the irradiation of several photon sources and exhibited a high dose enhancement spread out to about 30 μm from the GNP with low energy X-ray irradiation. Employing a similar method, Lin et al. indicated that the dose enhancement factor (DEF) under proton irradiation is up to 14 and is independent of the proton energy. Although these studies analyzed the dose enhancement range effectively, the radial dose distributions were given by concentric spherical shells defined around the GNP. This implies that the beam incident direction was not taken into account. Zygmanski et al. estimated the angular anisotropy of the DEF for a single GNP and reported that the dose enhancement is almost isotropic with 20 and 100 keV X-ray beams [20]. However, the energies of therapeutic protons are usually much higher than those of X-rays. This suggests that the spatial distribution of dose enhancement with proton beam irradiation will show different tendencies [21].

In this study, we calculated the radial dose distributions around the proton beam axis in the presence and absence of a GNP using the Geant4 Monte Carlo simulation toolkit. The dose enhancement caused by the GNP was evaluated by DEF (the ratio of dose with and without a GNP) and by D_{sub} (the subtracted difference between doses in the presence and absence of a GNP). The spatial DEF and D_{sub} distributions were calculated from the spatial dose distribution. To our knowledge, this is the first study to compare the dose enhancement among four depths around 100 and 195 MeV pristine proton Bragg peaks. The macroscopic dose enhancement within the tumor is also estimated in regard to GNP concentration.

2. Methods

2.1. General

Monte Carlo simulations of protons and electrons were performed using the Geant4 Monte Carlo simulation toolkit (version 4.10.0) [22]. The simulations were separated into two steps: a macroscopic step and a microscopic step. In the macroscopic step, the energy spectra of protons were determined at four depths in the absence of a GNP. In the microscopic step, protons with determined energy spectra were bombarded at the GNP by a point source in contact with the GNP and the energy depositions of the secondary electrons were calculated. This type of separation has already been attempted by several groups [18,20,23,24]. However, the present approach is partially different from those investigations in that proton bombardment to the GNP is simulated in the microscopic step and the radial dose distributions around the proton beam axis are calculated at a number of depths. In both steps, the proton sources were defined as point sources which emit the protons unidirectionally. This simplification enables us to investigate the radial dose distribution along the proton beam axis effectively.

2.2. Macroscopic step

In the macroscopic step, the energy spectra of a proton beam at four depths were calculated in the absence of a GNP. A 100 MeV and 195 MeV proton beam was incident on a cubic water phantom ($30 \times 30 \times 30$ cm). The proton beams were shot unidirectionally from a point source located at the border of the water phantom. The energy spectra of the protons were sampled in a 1 cm scoring cube positioned at four depths: 50% and 75% of maximum proximal to the Bragg peak, the Bragg peak, and 75% of maximum distal to the Bragg peak (denoted by P50, P75, Peak, and D75, respectively), as illustrated in Fig. 1(a). In scoring the spectra at the front surface of the scoring cube, the flux was normalized by the intensity of

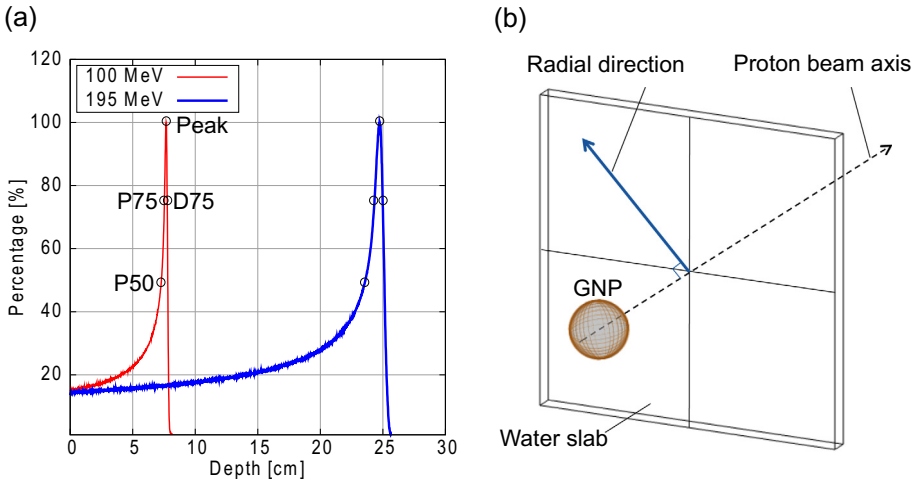

Fig. 1. (a) Schematic of the Bragg peak of 100 and 195 MeV protons. In the macroscopic step, the energy spectra of protons were calculated at four depths: for 50% and 75% of maximum proximal to the Bragg peak; for the Bragg peak; and for 75% of maximum distal to the Bragg peak (denoted by P50, P75, Peak, and D75, respectively). (b) Geometry for the sampling of energy deposition in the microscopic step. In this step, the radial dose distributions as a function of distance from the proton beam axis were obtained at every 1 nm depth behind the GNP.